eXPRESS Polymer Letters Vol.12, No.8 (2018) 688–698
Available online at www.expresspolymlett.com
https://doi.org/10.3144/expresspolymlett.2018.59

Facile approach to prepare pH and redox-responsive nanogels via Diels-Alder click reaction

C. M. Q. Le[1], *X. T. Cao*[2], *T. T. K. Tu*[1], *Y-S. Gal*[3], *K. T. Lim*[1*]

[1]Department of Display Engineering, Pukyong National University, Busan, South Korea
[2]Faculty of Chemical Engineering, Industrial University of Ho Chi Minh City, Vietnam
[3]Department of Fire Safety, Kyungil Univeristy, Gyeongsan City, Gyeongsangbuk-Do, South Korea

Received 8 January 2018; accepted in revised form 6 March 2018

Abstract. A novel pH and redox responsive system of sub-100 nm nanogels was prepared by arm-first approach via Diels-Alder click reaction. First, well-defined poly(ethylene glycol)-*block*-poly(styrene-*alt*-maleic anhydride) (PEG-*b*-PSM) was synthesized and subsequently functionalized with furfuryl amine, leading to the formation of the dual-functional block copolymer of PEG-*b*-PSMf. The furfuryl groups in the PSMf block were employed to incorporate a redox-responsive linkage and the carboxylic acid moieties generated through functionalization acted as a pH-responsive part. The Diels-Alder click reaction between a bismaleimide crosslinker and PEG-*b*-PSMf was conducted at 60 °C, affording star-like nanogel structures. Doxorubicin, a model anticancer drug, was loaded into to the core of the nanogels primarily by the ionic interaction with carboxylates of core blocks and a highest drug loading capacity of 38.1% was obtained. Furthermore, the *in vitro* profile showed a low release percentage (11.2%) of DOX at PBS pH 7.4, whereas a burst release (62%) at pH 5.0 in the presence of 10 mM glutathione, indicating the effective pH and redox responsive characteristic of the PEG-*b*-PSMf nanogels.

Keywords: *smart polymers, nanomaterials, nanogels, Diels-Alder click, drug delivery*

1. Introduction

Recently, polymeric nanogels have emerged as an interesting candidate in many areas of research, especially in material science and pharmacy, due to their diverse and suitable drug carrier properties [1–6]. Their outstanding properties include a high drug loading capacity, prolonged circulation period in the blood stream, and enhanced permeability, allowing efficient delivery of drug molecules to tumor site [7, 8]. Two approaches are commonly used for preparation of polymeric nanogels including physical and chemical crosslinking of preformed polymers [9–11]. Physical self-assembly in nanogel formation occurs via non-covalent attractive forces such as hydrophilic-hydrophilic, hydrophobic-hydrophobic, and ionic interactions, whereas chemical crosslinking can prevent dissolution of the hydrophilic polymer chains in aqueous media by covalent bonds [12]. Drug molecules can be efficiently loaded in nanogels before or after crosslinking process [13–15]. Cleavable crosslinks (e.g., ester, acetal, ketal, disulfide, hydrazine, amide, and anhydride bonds) are inserted either in cross-linkers or polymeric chains for allowing degradation of the nanogels network [16–18]. Recently, the Diels-Alder (DA) click reaction between maleimide and furan has attracted much attention for the design of crosslinked nanogels, since they can be efficiently carried out in water at low temperature without any catalyst and side-products [19–22]. On the other hand, the enhanced targeting of tumors by nanomedicines considerably depends on their size. The nanogels designed for anticancer drug delivery require a strict control of nanogel size in the range 10–200 nm to avoid fast excretion through kidney and target tumor

*Corresponding author, e-mail: ktlim@pknu.ac.kr

cells by 'enhanced permeability and retention' effect [23–27]. Therefore, it is desirable that polymeric nanogels are prepared using DA click chemistry together with degradable linkers, high drug loading, and favorable pharmacokinetics.

In this work, a novel pH and redox responsive drug release system of nanogels based on PEG-*b*-PSM was proposed by using DA click reaction (Figure 1). The block copolymers of PEG-*b*-PSM were synthesized by the reversible addition-fragmentation chain transfer (RAFT) polymerization. The high reactive maleic anhydride rings in PSM block was subsequently opened with furfuryl amine as a DA reactive group to form functional block copolymers (PEG-*b*-PSMf). On the other hand, the carboxylic acid groups generated in the PSMf block acted as pH-responsive moieties which enhanced the drug loading capacity via ionic interaction with a drug. The DA was allowed to occur between the PEG-*b*-PSMf and disulfide-based bismaleimide crosslinkers to form degradable nanogels. The formation of nanogels and its degradation was monitored by means of gel permeation chromatography (GPC). It is hypothesized that the nanogels would degrade in the high concentration of glutathione (GSH) and simultaneously squeeze out its cargo by protonation of carboxylic groups at low pH environment of cancer cells, which improves drug release efficiency. In this regard, doxorubicin (DOX) as a model drug was loaded into nanogels and *in vitro* drug release profile was investigated.

2. Experimental details

2.1. Materials

The PEG-RAFT macro-initiator was synthesized through the esterification reaction of poly(ethylene oxide) methyl ether and S-dodecyl-S′-(α,α′-dimethyl-α″-acetic acid) trithiocarbonate [28]. Maleic anhydride (≥99%), acetic anhydride (≥99%), triethylamine (99%), 1,4-dithiothreitol (DTT, 97%), and glutathione (97%) were purchased from Sigma-Aldrich (Korea). Doxorubicin hydrochloride (DOX.HCl) was kindly provided from Boryung Pharm. Co. (Korea). Styrene (99%, Alfa, Korea) was passed through a neutral alumina column and 2,2′-azobis(isobutyronitrile) (AIBN) (98%, Sigma-Aldrich, Korea) was recrystallized in methanol prior to use. Other solvents and chemicals of analytical grade were used as received. Dithiobismaleimidoethane (DTME) was synthesized as described in the previous work [29]. The crude compound was purified via column chromatography (ethyl acetate: hexane = 1:1). ^{1}H NMR (400 MHz, $CDCl_3$, δ ppm): 6.70 (m, 4H,

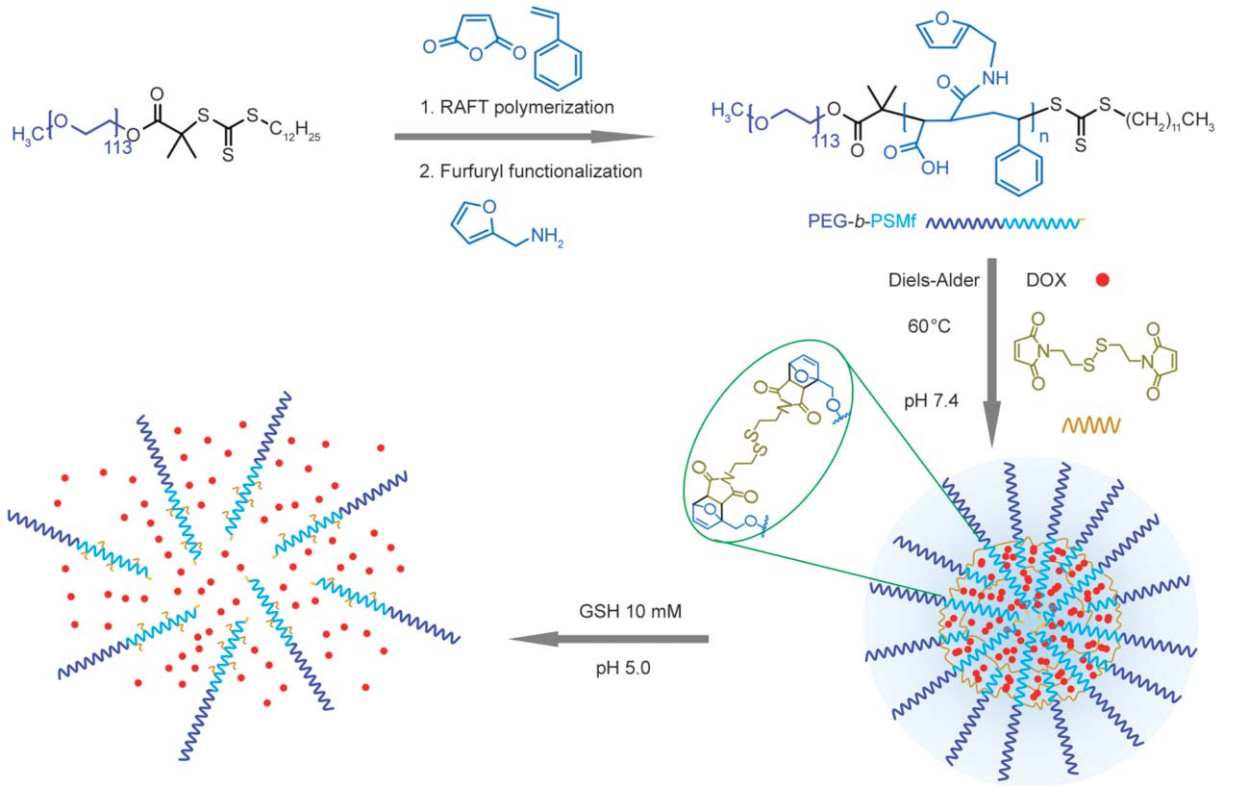

Figure 1. Synthesis of block copolymers of PEG-*b*-PSMf and the formation of nanogels followed by drug release in the presence of GSH 10 mM at pH 5.0.

–C***H***=C***H***–), 3.84 (t, J = 6.7 Hz, 4H, N–C***H***$_2$–CH$_2$), 2.92 (t, J = 6.7 Hz, 4H, –CH$_2$–C***H***$_2$–S).

2.2. Synthesis of block copolymers

PEG-*b*-PSM block copolymers were prepared by the RAFT method using the PEG-macro RAFT agent. In a typical procedure, PEG-macro RAFT (2.14 g, 0.4 mmol), maleic anhydride (1.96 g, 20 mmol), styrene (2.10 g, 20 mmol), AIBN (0.032 g, 0.2 mmol), and 1,4-dioxane (20 mL) were added into a round bottom flask, and purged with nitrogen for 1 h. The flask was placed in an oil bath under stirring at 60 °C for 16 h. The product was purified by precipitating the THF solution into excess hexane. The polymer was dried in a vacuum oven at 40 °C overnight (5.75 g, yield 92.7%).

In the next step, furfuryl amine (0.31 g, 3.1 mmol) was dissolved in DMF (6 mL) in a 20 mL round-bottom flask equipped with a Teflon-coated magnetic stirring bar. Then, PEG-*b*-PSM (1.0 g, 3.1 mmol maleic anhydride moieties) was added to the solution and the reaction mixture was placed in a preheated water bath of 50 °C. After stirring for 20 h, the mixture was cooled down to room temperature. The furfuryl functionalized block copolymer (PEG-*b*-PSMf) was purified by precipitation into diethyl ether. The final product was dried under vacuum at 40 °C for 24 h.

2.3. Nanogels formation and drug loading

A mixture of PEG-*b*-PSMf (60 mg, 0.14 mmol furfuryl moieties), DTME (22 mg, 0.07 mmol), and DMF (0.5 mL) was added into a 5 mL vial and the vial was placed in an oil bath at 60 °C. After 1.5 h of stirring the nanogels were cooled to room temperature and mixed with 9 mL of DOX.HCl solution (1.5 mg/mL in DMF). After 24 h of stirring in the dark, phosphate buffer saline (PBS) (pH 7.4, 10 mL, 10 mM) was added dropwise to the solution under vigorous stirring for 1 h. The mixture solution was transferred to the dialysis tubing and followed by dialysis against PBS (pH 7.4) to remove DMF and unloaded drugs. The amount of unloaded DOX in dialysis media was determined by UV-Visible spectroscopy at 485 nm. Drug loading capacity (DLC) and drug loading efficiency (DLE) were calculated by using Equations (1) and (2), respectively [30]:

$$\text{DLC}\,[\%] = \frac{(\text{The mass of DOX fed}) - (\text{The mass of unloaded DOX})}{(\text{The mass nanogels})} \cdot 100 \quad (1)$$

$$\text{DLE}\,[\%] = \frac{(\text{The mass of DOX fed}) - (\text{The mass of unloaded DOX})}{(\text{The mass of DOX fed})} \cdot 100 \quad (2)$$

2.4. *In vitro* drug release

3 mL of DOX loaded nanogels (1 mg/mL) was transferred in a dialysis bag (M_w cutoff, 13 kDa) and dialyzed against 20 mL of either PBS (0.01 M, pH 7.4) or acetate buffer solution (0.01 M, pH 5.0) with or without GSH at 37 °C. At selected time intervals, 3 mL of release media was taken out and the fresh one was then complemented. The amount of DOX release was measured using UV/visible spectroscopy at 485 nm. The experiments were carried out in triplicate and average values were taken.

2.5. Characterization

^{1}H NMR spectra were recorded on a JNM-ECP 400 (JEOL, Japan) instrument. GPC was performed using an HP 1100 (USA) apparatus equipped with three columns set PL gel 5 μm 10^4–10^3–10^2 Å. GPC was calibrated using polystyrene standards and *N,N′*-dimethylacetamide (DMAc) with 50 mM LiCl at 50 °C and flow rate of 1 mL/min. Fourier transform infrared (FTIR) spectra were measured on Cary640 (Agilent, USA) spectrometer in the 4000–500 cm^{-1} spectral region. For transmission electron microscopy (TEM; JEOL JEM-2010, Japan), the samples were coated on copper grids without staining. Dynamic laser light scattering (DLS) measurements were performed using ELS-8000 (Otsuka-Japan) with a He-Ne laser at a wavelength of 632.8 nm. The intensity of scattered light was detected at 90° to an incident beam. The elemental composition was performed on a vario Macro CHNS Element Analyzer (Germany) using sulfanilamide as a standard.

3. Results and discussion

3.1. Synthesis and characterization of block copolymers

To avoid a fast recognition by the immune system and prolong the blood circulation time of drug delivery system *in vivo*, PEG was used to construct block copolymers for nanogel preparation. In addition, styrene-*alt*-maleic anhydride copolymer (PSM) which has been proven to be biologically safe and favored for medical and pharmaceutical applications was designed as another part of the block copolymer. The selection of maleic copolymers as a functional block copolymer offers some advantages such as a

well-defined structure, the possibility to react with other chemical reagents under mild condition, and generation of carboxylic groups after being functionalized, which can form ionic bonding with cationic drugs [31–35]. Hence, the combination of PEG and PSM would be an optimal design for drug delivery system. In this study, poly(ethylene glycol)-*block*-poly(styrene-*alt*-maleic anhydride) (PEG-*b*-PSM) copolymers with different molecular weights were prepared by RAFT polymerization using PEG5000 as a macro-initiator. As summarized in Table 1, high conversions (>90%), well-defined molecular weights, and no residue of PEG macro-initiators in the product (Figure 2) indicated the controlled manner of the radical polymerization. The block copolymers were then functionalized with furfuryl amine through the ring opening reaction of maleic anhydride moieties. The successful functionalization reactions were examined by using GPC (Figure 2). The GPC graphs of PEG-*b*-PSMf showed a clear shift toward high molecular weight compared with its corresponding PEG-*b*-PSM.

The structure of amphiphilic block copolymers was confirmed by ^{1}H NMR spectroscopy as shown in Figure 3. In Figure 3 curve a, the main peaks of the dodecyl and methylene proton of the PEG-RAFT macro-initiator appeared at 1.22 and 3.6 ppm, respectively. The ^{1}H NMR spectrum of PEG-*b*-PSM showed the characteristic proton of phenyl rings at 6.5–7.6 ppm (Figure 3 curve b). The degree of polymerization was calculated by comparing the integration of phenyl groups and dodecyl groups. After modification of furfuryl amine, the spectrum of PEG-*b*-PSMf presented new characteristic peaks of furfuryl rings at 4.1, 6.2, 6.36 and 7.54 ppm (Figure 3 curve c). Furthermore, the synthesized block copolymers were characterized by FTIR spectroscopy as shown in Figure 4. In the spectrum of the PEG-RAFT macro initiator (Figure 4 curve a), a weak absorption band at 1734 cm^{-1} was attributed to the vibration of the carbonyl group of the RAFT agent moiety. The spectrum of PEG-*b*-PSM presented the characteristic peaks of anhydride groups at 1853 and 1780 cm^{-1}, and phenyl rings at 703 cm^{-1} verifying the existence of styrene and maleic anhydride in the block copolymer (Figure 4 curve b). After functionalization reaction, the spectrum of PEG-*b*-PSMf demonstrated the quantitative conversion of maleic anhydride groups by the complete disappearance of the peaks of anhydride groups at 1853 and 1780 cm^{-1} together with the presence of new peaks of amide groups at 1568, 1652 cm^{-1}, carboxylic groups at 1706 cm^{-1}, and furfuryl groups at 600 and 750 cm^{-1} (Figure 4 curve c).

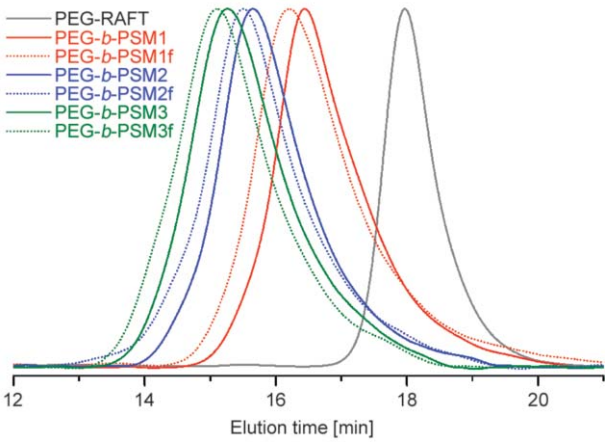

Figure 2. GPC chromatograms of block copolymers.

3.2. Nanogel formation by Diels-Alder reaction in non-selective solvent

To obtain nanogels with suitable size for drug delivery, we systematically investigated the effect of the molecular weight and concentration of the polymer and crosslinker on the nanogel formation by the mean of GPC, as shown in Figure 5 [36]. The GPC analysis of nanogels from copolymers with different molecular weights of PEG-*b*-PSM1f, PEG-*b*-PSM2f, and PEG-*b*-PSM3f (Table 1) showed a new peak at the lower retention time, indicating the formation of crosslinked nanogels (Figure 5a). Moreover, the gelation

Table 1. Characteristics of the PEG-*b*-PSM block copolymers prepared by RAFT polymerization.

Entry	Polymer	Feeding ratio[a] [S]/[MA]/[RAFT]	Conversion[b] [%]	$M_{n,\,Theo}$ [g·mol^{-1}]	$M_{n,\,NMR}$ [g·mol^{-1}]	PDI [GPC]
1	PEG-RAFT	–	–	5350	–	1.06
2	PEG-*b*-PSM1	50:50:1	92.7	14600	14200	1.21
3	PEG-*b*-PSM2	100:100:1	95.7	24700	24500	1.29
4	PEG-*b*-PSM3	150:150:1	98.0	35000	34800	1.39

[a]Polymerization was carried out at 60 °C for 16 h. Molar ratio [PEG-RAFT]: [AIBN] = 2:1.
[b] Conversion was determined gravimetrically.

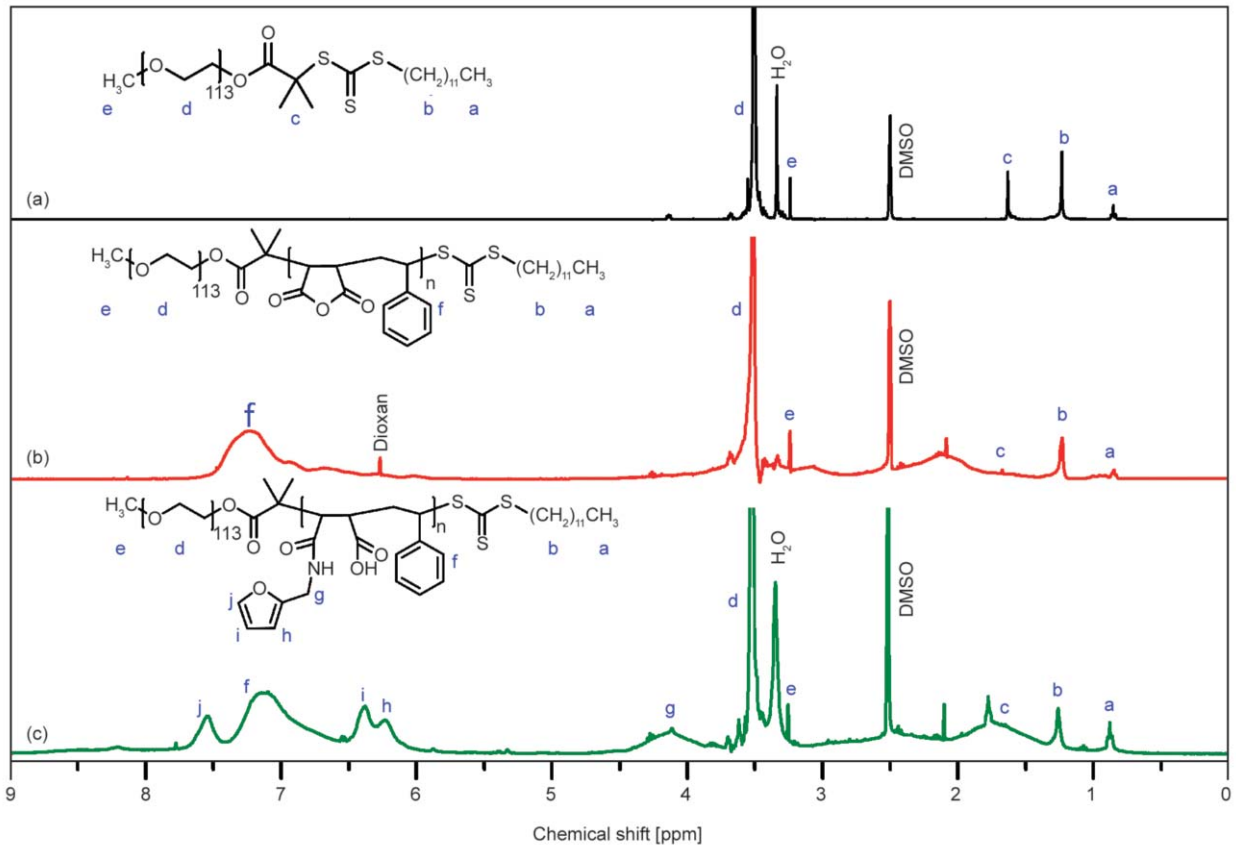

Figure 3. ^{1}H NMR spectra of (a) PEG-RAFT macro-initiator, (b) PEG-*b*-PSM, and (c) PEG-*b*-PSMf.

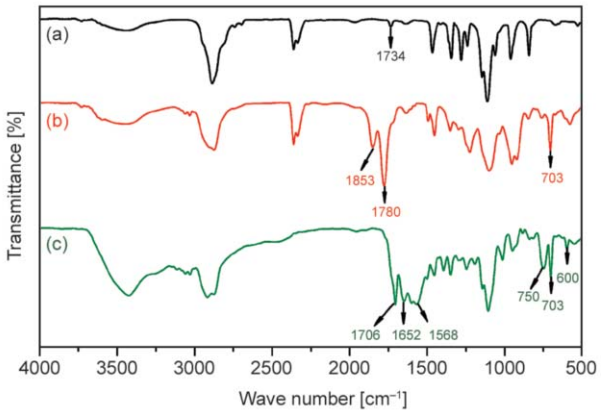

Figure 4. FT-IR spectra of (a) PEG-RAFT macro initiator, (b) PEG-*b*-PSM, and (c) PEG-*b*-PSMf.

time became shorter as the molecular weight of PEG-*b*-PSMf decreased. The formation of gels was observed by the crosslinking reaction of PEG-*b*-PSM1f after only 2 h and it turned into solid state after 30 min more. In contrast to PEG-*b*-PSM1f, the cross-linking reaction of PEG-*b*-PSM2f and PEG-*b*-PSM3f remained viscous liquid after 24 h. Therefore, PEG-*b*-PSM1f block was chosen for further investigation.

At the molar ratio of 1:1 of furan/maleimide, the cross-linking reaction was performed at three different polymer concentrations of 120, 30, and 60 mg/mL, as shown in Figure 5b, 5c, and 5e, respectively. As seen in GPC traces, higher concentrations resulted in faster rates of gelation. However, the star-star coupling reaction of nanogels at high concentration (120 mg/mL) led to the formation of macrogels which are undesirable (Figure 5b). On the other hand, the GPC graphs of nanogels at 30 and 60 mg/mL (Figure 5c and 5e) were relatively narrow but the gelation rate was slow. The rate of nanogel formation was also examined at three different amounts of the bismaleimide crosslinker. Similarly, the gelation rate became faster as the crosslinker concentration increased (Figure 5d, 5e, and 5f). It can be considered that the number of residual arms and star-star coupling could be significantly reduced at the molar ratio of 1:1 of furan/maleimide compared to that of 1:0.5 and 1:2. Therefore, the nanogel samples prepared from the molar ratio of 1:1 were used to analyze the size distribution and morphology by TEM and DLS. The average size of crosslinked nanogels was smaller than 100 nm in drying regime (Figure 6a) and around 100 nm in swelling state (Figure 6b), which could be suitable for anticancer drug delivery [37, 38].

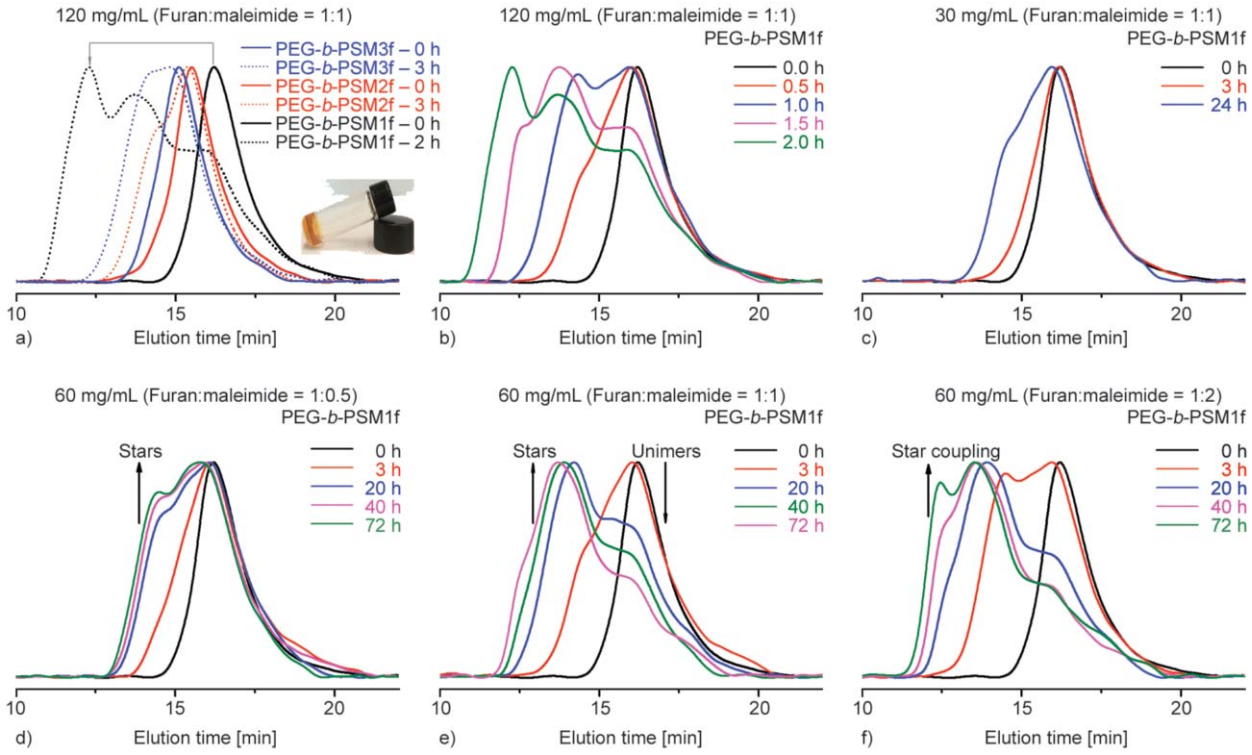

Figure 5. GPC traces of the nanogel formation in DMF at different molecular weights and concentrations of block copolymers, and molar ratios of furan groups to maleimide groups (Furan:maleimide). The progress of nanogel formation at a) different molecular weight, [polymer] = 120 mg/mL, molar ratio of furan:maleimide = 1:1; b) [PEG-*b*-PSM1f] = 120 mg/mL, molar ratio of furan:maleimide = 1:1; c) [PEG-b-PSM1f] = 30 mg/mL, molar ratio of furan:maleimide = 1:1; d) [PEG-*b*-PSM1f] = 60 mg/mL, molar ratio of furan:maleimide = 1:0.5; e) [PEG-*b*-PSM1f] = 60 mg/mL, molar ratio of furan:maleimide = 1:1; f) [PEG-*b*-PSM1f] = 60 mg/mL, molar ratio of furan:maleimide = 1:2.

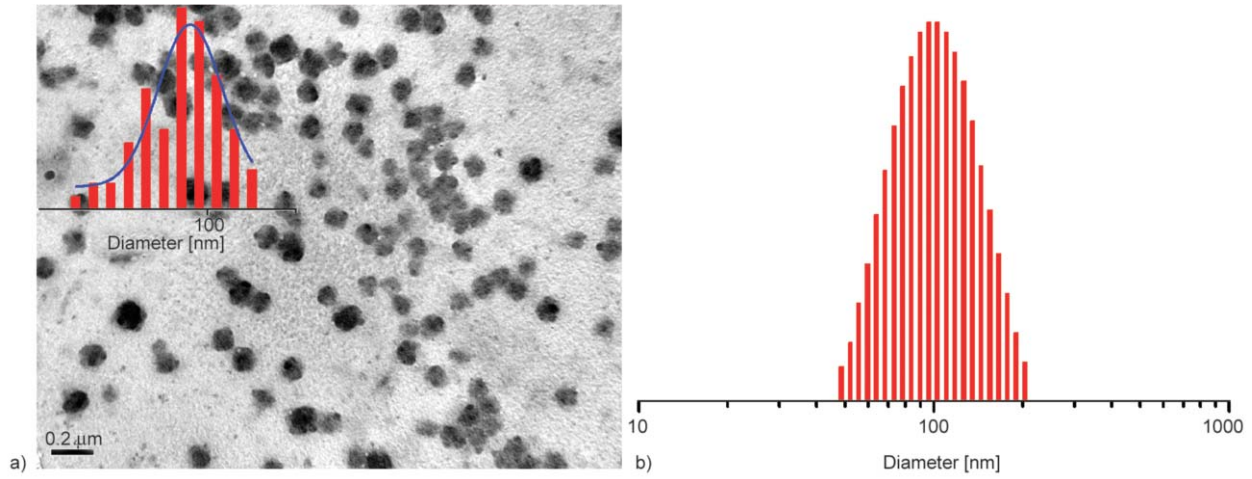

Figure 6. The TEM image and DLS result of cross-linked nanogels: a) TEM image and their size distribution (inset), b) size distribution measured by DLS .

The selected nanogels formed at the condition of 120 mg/mL, furan:maleimide molar ratio = 1:1 and 1.5 h was isolated by dilution with THF and precipitated in diethyl ether. After drying at 40 °C under vacuum, the degree of crosslinking was determined by using elemental analysis to observe the sulfur content originated from the crosslinker [14]. The result is summarized in Table 2. Assuming that 100% of crosslinker is incorporated in the nanogels, the degree of crosslinking was evaluated to be 93% by

Table 2. Elemental composition of nanogels.

	N [%]	C [%]	H [%]	S [%]
Theoretical calculation	4.83	59.20	6.23	5.90
Measurement	5.14	58.76	5.94	5.49

comparing the sulfur content from theoretical calculation and experimental measurement. The result demonstrates the high efficiency of DA reaction in forming crosslinked nanogels.

Nanogel degradation

Nanogels (5.0 mg) were dispersed in PBS buffer (10 mL, pH 7.4) in the presence of 10 mM DTT or GSH as a reducing agent in order to investigate whether nanogels degrade under the reducing condition. The mixture was incubated at 37 °C for 24 h. The solvent was exchanged to DMAc, filtered through 0.45 µm and analyzed by GPC system [39]. In Figure 7, GPC traces show a clear shift to higher retention times of nanogels after incubation. This is attributed to the cleavage of disulfide-based crosslinking in nanogels under reducing circumstance, which led to the degradation of the nanogel network into lower molecular weight polymer chains. This result indicates that the disulfide linkage in nanogels could be effectively cleaved in the presence of a reducing agent.

In order to investigate the pH and redox-responsive ability, the particle size change of nanogels at different pH values and in the presence of glutathione were studied. As shown in Figure 8, the average size of nanogels in distilled water is 105 nm. The nanogels underwent slightly swelling to 108 nm when the pH was adjusted to pH 7.4. In contrast, the nanogel size decreases slightly to 100 nm when the pH was brought down to pH 5.0. This phenomenon could be attributed to the pH sensitivity of the nanogels, which is mainly related to the protonation and deprotonation of carboxylic groups in the nanogels. Following the addition of GSH 10 mM at pH 5, the diameter of nanogels expanded to 215 nm due to the cleavage of disulfide crosslinking bonds. These results coincide with the stability of nanogels from GPC results, demonstrating the successful fabrication of pH and redox responsive nanogels [40]

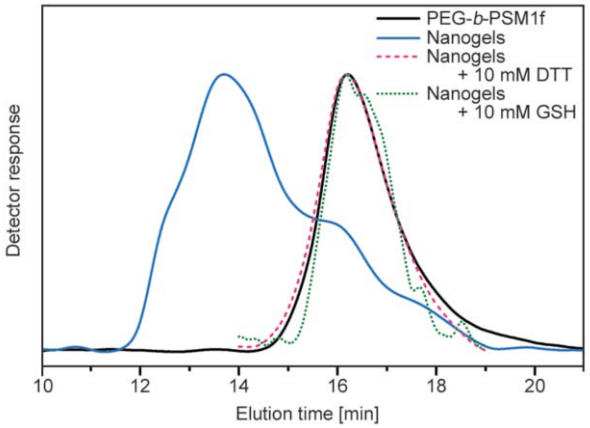

Figure 7. GPC traces showing nanogels degradation.

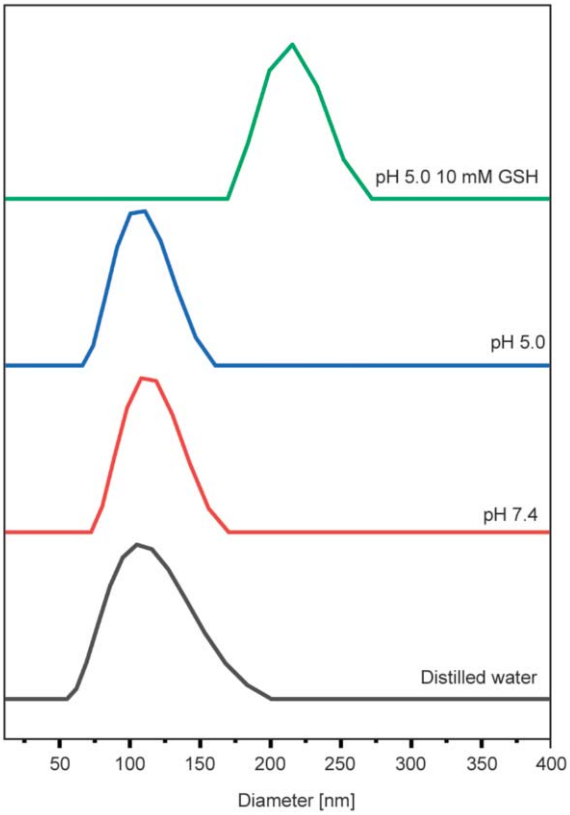

Figure 8. pH and GSH-induced size change of nanogels.

Drug loading and in vitro drug release

In this study, drug loading was examined at various drug feeding ratios. As shown in Table 3, the nanogels displayed a high drug loading capacity and achieved 38.1% level of DLC. The high loading of DOX into nanogels can be largely attributed to two factors: the ionic interaction between carboxylate groups in the polymer and amine groups in DOX [41, 42]; the hydrophobic interaction between phenyl rings in both polymer and DOX [43]. The cooperativity of the ionic and hydrophobic interactions could significantly enhance the drug loading capacity. In comparison with core crosslinked micelles without carboxylic and phenyl groups from previous report [28], the DLC was considerably enhanced. However, DLE was

Table 3. DLC and DLE at different drug feed ratios.

DOX-nanogel	Drug feeding [wt%]	DLC [wt%]	DLE [wt%]
1	18.2	14.5	76.3
2	25.0	19.7	73.7
3	40.0	31.2	67.9
4	50.0	38.1	61.7

decreased when drug feeding ratios were increased. By evaluating the balance between DLE and DLC, the nanogels with 18.2% of drug feeding were used for testing the *in vitro* drug release.

The pH and redox responsive behaviors of nanogels were studied by the *in vitro* drug release with pH 5.0 of acetate buffer (representing the intracellular pH of cancer cells) and pH 7.4 of PBS solution (representing the pH of physiological environment) in the presence or absence of a reducing agent. The drug release profile was studied using a dialysis method and shown in Figure 8. In the absence of GSH, DOX cumulative release from nanogels was about 11.2% at pH 7.4 after 72 h (Figure 9 curve a). The nanogels present a low premature drug release at physiological pH condition due to the stability of the crosslinked structure. As compared to pH 7.4, DOX was released at a higher rate at pH 5.0 (Figure 9 curve b). This observation could be explained from the fact that the increase in solubility of DOX at low pH results in the faster diffusion of DOX and the protonation of the carboxylate groups at low pH increases hydrophobic effects [44, 45]. Consequently, DOX released from nanogels at pH 5.0 was about 24.4% after 72 h, which was more than double the DOX release at pH 7.4. These results demonstrated pH-sensitive drug release of the nanogels.

Moreover, DOX release was found to be significantly enhanced in the presence of the reducing agent, GSH. In this experiment, GSH was used as a reducing agent because it is spontaneously produced at high concentration in cancer cells. Hence, the use of GSH could reflect more accurate drug release profile as compare with DTT [46, 47]. A concentration of 10 mM GSH was chosen to simulate the cytoplasmic concentration of GSH in cancer cells [48, 49]. The addition of 10 mM GSH in both pH 5.0 and pH 7.4 greatly enhanced the rate of DOX release (Figure 9 curve c and d), demonstrating that the nanogels exhibited the redox-responsive characteristic. Interestingly, the response of nanogels to GSH was more significant than acidic pH. This phenomenon may be explained by the fact that GSH is not only act as a reducing agent but also play a role in displacing the ionic bond between carboxylate groups of the nanogels and the amino groups of DOX, thus enhancing the rate of DOX release [46]. Accordingly, the highest drug release of 62% at 72 h was obtained when the dual stimuli pH-redox responsive condition was applied (Figure 9 curve d).

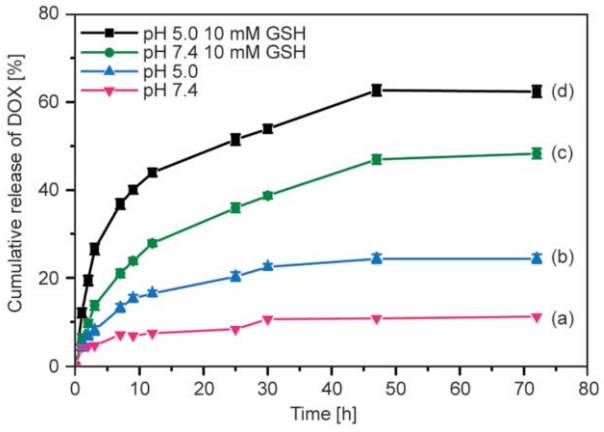

Figure 9. Cumulative DOX release from the nanogels.

4. Conclusions

In summary, novel pH and redox-responsive nanogels based on the block copolymer of PEG-*b*-PSMf were prepared via RAFT polymerization and DA click reaction. Block copolymers and the formation of nanogels were characterized by ^{1}H NMR, FT-IR, and GPC analysis. The nanogels were finely tuned to obtain a suitable size (~100 nm) which could have potential application in drug delivery system. The obtained nanogels showed high drug loading with 14.5% of DLC and 76.3% of DLE possibly thanks to the interaction between DOX and PSMf cores of the nanogels. Moreover, the DOX loaded nanogels possessed dual pH-redox triggered behavior with high drug release rate (62%) at tumor intracellular environment (pH 5.0 and 10 mM GSH) whereas they maintained low release rate (11.2%) at physiological condition after 72 h.

Acknowledgements

This work was supported by the National Research Foundation of Korea (NRF) Grant funded by the Ministry of Education (NRF-2015R1D1A3A01019109).

References

[1] Ekkelenkamp A. E., Elzes M. R., Engbersen J. F. J., Paulusse J. M. J.: Responsive crosslinked polymer nanogels for imaging and therapeutics delivery. Journal of Materials Chemistry B, **6**, 210–235 (2018). https://doi.org/10.1039/c7tb02239e

[2] Soni G., Yadav K. S.: Nanogels as potential nanomedicine carrier for treatment of cancer: A mini review of the state of the art. Saudi Pharmaceutical Journal, **24**, 133–139 (2016). https://doi.org/10.1016/j.jsps.2014.04.001

[3] Wu H-Q., Wang C-C.: Biodegradable smart nanogels: A new platform for targeting drug delivery and biomedical diagnostics. Langmuir, **32**, 6211–6225 (2016). https://doi.org/10.1021/acs.langmuir.6b00842

[4] Cao X. T., Showkat A. M., Lim K. T.: Synthesis of nanogels of poly(ε-caprolactone)-*b*-poly(glycidyl methacrylate) by click chemistry in direct preparation. European Polymer Journal, **68**, 267–277 (2015). https://doi.org/10.1016/j.eurpolymj.2015.04.025

[5] Molina M., Asadian-Birjand M., Balach J., Bergueiro J., Miceli E., Calderón M.: Stimuli-responsive nanogel composites and their application in nanomedicine. Chemical Society Reviews, **44**, 6161–6186 (2015). https://doi.org/10.1039/c5cs00199d

[6] Cheng R., Meng F., Deng C., Klok H-A., Zhong Z.: Dual and multi-stimuli responsive polymeric nanoparticles for programmed site-specific drug delivery. Biomaterials, **34**, 3647–3657 (2013). https://doi.org/10.1016/j.biomaterials.2013.01.084

[7] Teo J. Y., Chin W., Ke X., Gao S., Liu S., Cheng W., Hedrick J. L., Yang Y. Y.: pH and redox dual-responsive biodegradable polymeric micelles with high drug loading for effective anticancer drug delivery. Nanomedicine: Nanotechnology, Biology and Medicine, **13**, 431–442 (2017). https://doi.org/10.1016/j.nano.2016.09.016

[8] Hamzah Y. B., Hashim S., Rahman W. A. W. A.: Synthesis of polymeric nano/microgels: A review. Journal of Polymer Research, **24**, 134/1–139/19 (2017). https://doi.org/10.1007/s10965-017-1281-9

[9] Soni K. S., Desale S. S., Bronich T. K.: Nanogels: An overview of properties, biomedical applications and obstacles to clinical translation. Journal of Controlled Release, **240**, 109–126 (2016). https://doi.org/10.1016/j.jconrel.2015.11.009

[10] Sekine Y., Endo H., Iwase H., Takeda S., Mukai S-A., Fukazawa H., Littrell K. C., Sasaki Y., Akiyoshi K.: Nanoscopic structural investigation of physically cross-linked nanogels formed from self-associating polymers. The Journal of Physical Chemistry B, **120**, 11996–12002 (2016). https://doi.org/10.1021/acs.jpcb.6b06795

[11] Aktan B., Chambre L., Sanyal R., Sanyal A.: 'Clickable' nanogels via thermally driven self-assembly of polymers: Facile access to targeted imaging platforms using thiol–maleimide conjugation. Biomacromolecules, **18**, 490–497 (2017). https://doi.org/10.1021/acs.biomac.6b01576

[12] Cao X. T., Kim Y. H., Park J. M., Lim K. T.: One-pot syntheses of dual-responsive core cross-linked polymeric micelles and covalently entrapped drug by click chemistry. European Polymer Journal, **78**, 264–273 (2016). https://doi.org/10.1016/j.eurpolymj.2016.03.039

[13] Zhang Y., Zhou J., Yang C., Wang W., Chu L., Huang F., Liu Q., Deng L., Kong D., Liu J., Liu J.: Folic acid-targeted disulfide-based cross-linking micelle for enhanced drug encapsulation stability and site-specific drug delivery against tumors. International Journal of Nanomedicine, **11**, 1119–1130 (2016). https://doi.org/10.2147/IJN.S101649

[14] Park C. W., Yang H-M., Woo M-A., Lee K. S., Kim J-D.: Completely disintegrable redox-responsive poly(amino acid) nanogels for intracellular drug delivery. Journal of Industrial and Engineering Chemistry, **45**, 182–188 (2017). https://doi.org/10.1016/j.jiec.2016.09.021

[15] Cao X. T., Le C. M. Q., Thi H. H. P., Kim G-D., Gal Y-S., Lim K. T.: Redox-responsive core cross-linked prodrug micelles prepared by click chemistry for pH-triggered doxorubicin delivery. Express Polymer Letters, **11**, 832–845 (2017). https://doi.org/10.3144/expresspolymlett.2017.79

[16] Liu B., Thayumanavan S.: Substituent effects on the pH sensitivity of acetals and ketals and their correlation with encapsulation stability in polymeric nanogels. Journal of the American Chemical Society, **139**, 2306–2317 (2017). https://doi.org/10.1021/jacs.6b11181

[17] Zhang X., Malhotra S., Molina M., Haag R.: Micro- and nanogels with labile crosslinks – From synthesis to biomedical applications. Chemical Society Reviews, **44**, 1948–1973 (2015). https://doi.org/10.1039/c4cs00341a

[18] Hrubý M., Filippov S. K., Štěpánek P.: Smart polymers in drug delivery systems on crossroads: Which way deserves following? European Polymer Journal, **65**, 82–97 (2015). https://doi.org/10.1016/j.eurpolymj.2015.01.016

[19] Altinbasak I., Sanyal R., Sanyal A.: Best of both worlds: Diels–Alder chemistry towards fabrication of redox-responsive degradable hydrogels for protein release. RSC Advances, **6**, 74757–74764 (2016). https://doi.org/10.1039/c6ra16126j

[20] Li S., Wang L., Yu X., Wang C., Wang Z.: Synthesis and characterization of a novel double cross-linked hydrogel based on Diels–Alder click reaction and coordination bonding. Materials Science and Engineering: C, **82**, 299–309 (2018). https://doi.org/10.1016/j.msec.2017.08.031

[21] Gregoritza M., Messmann V., Abstiens K., Brandl F. P., Goepferich A. M.: Controlled antibody release from degradable thermoresponsive hydrogels cross-linked by Diels–Alder chemistry. Biomacromolecules, **18**, 2410–2418 (2017). https://doi.org/10.1021/acs.biomac.7b00587

[22] Buwalda S. J., Vermonden T., Hennink W. E.: Hydrogels for therapeutic delivery: Current developments and future directions. Biomacromolecules, **18**, 316–330 (2017). https://doi.org/10.1021/acs.biomac.6b01604

[23] Choi H. S., Liu W., Misra P., Tanaka E., Zimmer J. P., Itty Ipe B., Bawendi M. G., Frangioni J. V.: Renal clearance of quantum dots. Nature Biotechnology, **25**, 1165–1170 (2007). https://doi.org/10.1038/nbt1340

[24] Fang J., Nakamura H., Maeda H.: The EPR effect: Unique features of tumor blood vessels for drug delivery, factors involved, and limitations and augmentation of the effect. Advanced Drug Delivery Reviews, **63**, 136–151 (2011). https://doi.org/10.1016/j.addr.2010.04.009

[25] Cabral H., Matsumoto Y., Mizuno K., Chen Q., Murakami M., Kimura M., Terada Y., Kano M. R., Miyazono K., Uesaka M., Nishiyama N., Kataoka K.: Accumulation of sub-100 nm polymeric micelles in poorly permeable tumours depends on size. Nature Nanotechnology, **6**, 815–823 (2011). https://doi.org/10.1038/nnano.2011.166

[26] Chen H., Zhang W., Zhu G., Xie J., Chen X.: Rethinking cancer nanotheranostics. Nature Reviews Materials, **2**, 17024/1–17024/19 (2017). https://doi.org/10.1038/natrevmats.2017.24

[27] Movassaghian S., Merkel O. M., Torchilin V. P.: Applications of polymer micelles for imaging and drug delivery. Wire's Nanomedicine and Nanobiotechnology, **7**, 691–707 (2015). https://doi.org/10.1002/wnan.1332

[28] Le C. M. Q., Thi H. H. P., Cao X. T., Kim G-D., Oh C-W., Lim K. T.: Redox-responsive core cross-linked micelles of poly(ethylene oxide)-*b*-poly(furfuryl methacrylate) by Diels–Alder reaction for doxorubicin release. Journal of Polymer Science Part A: Polymer Chemistry, **54**, 3741–3750 (2016). https://doi.org/10.1002/pola.28271

[29] Dispinar T., van Camp W., de Cock L. J., de Geest B. G., du Prez F. E.: Redox-responsive degradable PEG cryogels as potential cell scaffolds in tissue engineering. Macromolecular Bioscience, **12**, 383–394 (2012). https://doi.org/10.1002/mabi.201100396

[30] Zhang X., Liang X., Gu J., Chang D., Zhang J., Chen Z., Ye Y., Wang C., Tao W., Zeng X., Liu G., Zhang Y., Mei L., Gu Z.: Investigation and intervention of autophagy to guide cancer treatment with nanogels. Nanoscale, **9**, 150–163 (2017). https://doi.org/10.1039/c6nr07866d

[31] Popescu I., Suflet D. M., Pelin I. M.: Biomedical applications of maleic anhydride copolymers. Revue Roumaine de Chimie, **56**, 173–188 (2011).

[32] Moghadam P. N., Azaryan E., Zeynizade B.: Investigation of poly(styrene-alt-maleic anhydride) copolymer for controlled drug delivery of ceftriaxone antibiotic. Journal of Macromolecular Science Part A: Pure and Applied Chemistry, **47**, 839–848 (2010). https://doi.org/10.1080/10601325.2010.492265

[33] Larson N., Greish K., Bauer H., Maeda H., Ghandehari H.: Synthesis and evaluation of poly(styrene-*co*-maleic acid) micellar nanocarriers for the delivery of tanespimycin. International Journal of Pharmaceutics, **420**, 111–117 (2011). https://doi.org/10.1016/j.ijpharm.2011.08.011

[34] Pompe T., Zschoche S., Herold N., Salchert K., Gouzy M. F., Sperling C., Werner C.: Maleic anhydride copolymers – A versatile platform for molecular biosurface engineering. Biomacromolecules, **4**, 1072–1079 (2003). https://doi.org/10.1021/bm034071c

[35] Amirmahani N., Mahmoodi N. O., Mohammadi Galangash M., Ghavidast A.: Advances in nanomicelles for sustained drug delivery. Journal of Industrial and Engineering Chemistry, **55**, 21–34 (2017). https://doi.org/10.1016/j.jiec.2017.06.050

[36] Bapat A. P., Ray J. G., Savin D. A., Hoff E. A., Patton D. L., Sumerlin B. S.: Dynamic-covalent nanostructures prepared by Diels–Alder reactions of styrene-maleic anhydride-derived copolymers obtained by one-step cascade block copolymerization. Polymer Chemistry, **3**, 3112–3120 (2012). https://doi.org/10.1039/c2py20351k

[37] Storm G., Belliot S. O., Daemen T., Lasic D. D.: Surface modification of nanoparticles to oppose uptake by the mononuclear phagocyte system. Advanced Drug Delivery Reviews, **17**, 31–48 (1995). https://doi.org/10.1016/0169-409x(95)00039-a

[38] Milani A. H., Saunders J. M., Nguyen N. T., Ratcliffe L. P. D., Adlam D. J., Freemont A. J., Hoyland J. A., Armes S. P., Saunders B. R.: Synthesis of polyacid nanogels: pH-responsive sub-100 nm particles for functionalisation and fluorescent hydrogel assembly. Soft Matter, **13**, 1554–1560 (2017). https://doi.org/10.1039/c6sm02713j

[39] Wu H., Jin H., Wang C., Zhang Z., Ruan H., Sun L., Yang C., Li Y., Qin W., Wang C.: Synergistic cisplatin/doxorubicin combination chemotherapy for multidrug-resistant cancer via polymeric nanogels targeting delivery. ACS Applied Materials and Interfaces, **9**, 9426–9436 (2017). https://doi.org/10.1021/acsami.6b16844

[40] Wang L., Zhang J., Song M., Tian B., Li K., Liang Y., Han J., Wu Z.: A shell-crosslinked polymeric micelle system for pH/redox dual stimuli-triggered dox on-demand release and enhanced antitumor activity. Colloids and Surfaces B: Biointerfaces, **152**, 1–11 (2017). https://doi.org/10.1016/j.colsurfb.2016.12.032

[41] Jin S., Li D., Yang P., Guo J., Lu J. Q., Wang C.: Redox/pH stimuli-responsive biodegradable PEGylated p(MAA/BACy) nanohydrogels for controlled releasing of anticancer drugs. Colloids and Surfaces A: Physicochemical and Engineering Aspects, **484**, 47–55 (2015). https://doi.org/10.1016/j.colsurfa.2015.07.041

[42] Cuggino J. C., Molina M., Wedepohl S., Igarzabal C. I. A., Calderón M., Gugliotta L. M.: Responsive nanogels for application as smart carriers in endocytic pH-triggered drug delivery systems. European Polymer Journal, **78**, 14–24 (2016). https://doi.org/10.1016/j.eurpolymj.2016.02.022

[43] Baranello M. P., Bauer L., Benoit D. S.: Poly(styrene-*alt*-maleic anhydride)-based diblock copolymer micelles exhibit versatile hydrophobic drug loading, drug-dependent release, and internalization by multidrug resistant ovarian cancer cells. Biomacromolecules, **15**, 2629–2641 (2014). https://doi.org/10.1021/bm500468d

[44] Zhao X., Liu P.: Reduction-responsive core–shell–corona micelles based on triblock copolymers: Novel synthetic strategy, characterization, and application as a tumor microenvironment-responsive drug delivery system. ACS Applied Materials and Interfaces, **7**, 166–174 (2015). https://doi.org/10.1021/am505531e

[45] Guo M., Yan Y., Zhang H., Yan H., Cao Y., Liu K., Wan S., Huang J., Yue W.: Magnetic and pH-responsive nanocarriers with multilayer core–shell architecture for anticancer drug delivery. Journal of Materials Chemistry, **18**, 5104–5112 (2008). https://doi.org/10.1039/b810061f

[46] Pan Y-J., Chen Y-Y., Wang D-R., Wei C., Guo J., Lu D-R., Chu C-C., Wang C-C.: Redox/pH dual stimuli-responsive biodegradable nanohydrogels with varying responses to dithiothreitol and glutathione for controlled drug release. Biomaterials, **33**, 6570–6579 (2012). https://doi.org/10.1016/j.biomaterials.2012.05.062

[47] Talelli M., Barz M., Rijcken C. J., Kiessling F., Hennink W. E., Lammers T.: Core-crosslinked polymeric micelles: Principles, preparation, biomedical applications and clinical translation. Nano Today, **10**, 93–117 (2015). https://doi.org/10.1016/j.nantod.2015.01.005

[48] Mura S., Nicolas J., Couvreur P.: Stimuli-responsive nanocarriers for drug delivery. Nature Materials, **12**, 991–1003 (2013). https://doi.org/10.1038/nmat3776

[49] Cheng R., Feng F., Meng F., Deng C., Feijen J., Zhong Z.: Glutathione-responsive nano-vehicles as a promising platform for targeted intracellular drug and gene delivery. Journal of Controlled Release, **152**, 2–12 (2011). https://doi.org/10.1016/j.jconrel.2011.01.030